

Nonspecific Cation Current Associated with Native Polycystin-2 in HEK-293 Cells

Bruna Pelucchi,* Gianluca Aguiari,[†] Angela Pignatelli,* Elisa Manzati,[†] Ralph Witzgall,[‡] Laura del Senno,[†] and Ottorino Belluzzi*

Departments of *Biology and [†]Biochemistry and Molecular Biology, University of Ferrara, Ferrara, Italy; and [‡]Institute for Molecular and Cellular Anatomy, University of Regensburg, Regensburg, Germany

Mutations in either *PKD1* or *PKD2* gene are associated with autosomal dominant polycystic kidney disease, the most common inherited kidney disorder. Polycystin-2 (PC2), the *PKD2* gene product, and the related protein polycystin-L, function as Ca²⁺-permeable, nonselective cation channels in different expression systems. This work describes a nonspecific cation current (I_{CC}) that is present in native HEK-293 cells and highly associated with a PC2-channel activity. The current is voltage dependent, activating for potentials that are positive to -50 mV and inactivating in a few milliseconds. It is sensitive to Cd²⁺, Gd³⁺, La³⁺, SKF96365, and amiloride. After silencing of PC2 by RNA interfering, cells show a reduced current that is restored by transfection with normal but not truncated PC2. Consistently, I_{CC} is abolished by perfusion with an anti-PC2 antibody. Furthermore, heterologous expression of the PC1 cytoplasmic tail significantly increases I_{CC} peak amplitude compared with native cells. This is the first characterization of such a current in HEK-293 cells, a widely used expression system for ion channels. These cells, therefore, could be regarded as a suitable and readily accessible tool to study interactions between native PC2/PC1 complex and other membrane proteins, thus contributing to the understanding of autosomal dominant polycystic kidney disease pathogenesis.

J Am Soc Nephrol 17: 388–397, 2006. doi: 10.1681/ASN.2004121146

Autosomal dominant polycystic kidney disease (ADPKD) accounts for approximately 10% of all cases of ESRD (1). Two genes are involved in ADPKD pathogenesis: *PKD1* and *PKD2* (2,3), and mutations in either cause virtually the same clinical picture.

Since the characterization of the two gene products, PC1 and PC2, further homologous proteins have been identified, but their role in ADPKD pathogenesis is not yet clear. According to sequence similarities, they are classified in PC1-like (PC1, PC1L2, PC1L3, and PCREJ) and PC2-like (PC2, PCL, and PC2L2) proteins.

PC1 is an integral plasma membrane glycoprotein that has a large extracellular N-terminal domain, up to 11 transmembrane domains, and a relatively short intracellular carboxyl tail (4) and has been shown to interact functionally with the C-terminus of PC2 and other proteins (5). PC2 and PCL are voltage-dependent, Ca²⁺-modulated, nonselective cation channels (6–11), with a moderate homology with TRP channels and voltage-activated Ca²⁺ and Na⁺ channels (12).

In this study, we demonstrate that HEK-293 cells express a novel voltage-dependent inactivating inward current, highly

associated with, if not sustained by, PC2-channel activities. To our knowledge, this is the first electrophysiologic evidence for such a current in native HEK-293 cells. Therefore, native HEK-293 cells could be regarded as an alternative and readily accessible model to study interactions between PC1 and PC2 and other putative partners, in experimental conditions that are unaltered by heterologous expression, thereby contributing to a better understanding of ADPKD pathogenesis. Furthermore, these data suggest that great precaution should be taken when this widely used expression system is used to study similar ion channels.

Materials and Methods

DNA Constructs and Cell Lines

For silencing *PKD2* gene expression, two oligonucleotides (F, 5'-GATCCCC-TGTGGAGGTGCTACTACAGTTC AAGAGACTGTAGTAGCACCTCCAC-ATTTTGGAAA3' and R, 5'-AGCTTTTCCAAAAATGTTGGAGGTGCTACTACAGTCTCTTGAAGTGTAGTAGCACCTCCACAGGG3') that contain the underlined *PKD2* cDNA sequence, localized at nt + 1659 (NM-000297), were cloned in pSuper vector expression system (Oligoengine, Seattle, WA). The recombinant vector was co-transfected (ratio 1:10) with the G418 antibiotic-resistance pCDNA3 vector (Invitrogen C, Carlsbad, CA) in HEK-293 cells. After 3 wk of selection, stable HEK^{PKD2-} clones (WTPC2⁻) and HEK^{pSuper} control clones were isolated. WTPC2⁻ cells were transiently transfected with plasmids that express a green fluorescence protein-tagged full-length PC2 (FLPC2) and, as control, hemagglutinin-tagged PC2 truncated at codon 604 in loop 4 (PC2stop), with the Ca²⁺ phosphate precipitation (13,14). PC2 expression was detected by Western blot analysis by using the anti-N-terM anti-PC2 antibody, purified by immunoaffinity against its peptide as described previously (13). In immunofluorescence experiments, cells were cultured on 24-mm

Received December 29, 2004. Accepted November 21, 2005.

Published online ahead of print. Publication date available at www.jasn.org.

B.P. and G.A. equally contributed to this work.

Address correspondence to: Dr. Bruna Pelucchi, University of Ferrara, Department of Biology, Via L. Borsari 46, Ferrara I-44100, Italy. Phone: +39-0532-291485; Fax: +39-0532-207143; E-mail: plb@dns.unife.it

coverslips for 24 h. After two washes with PBS buffer, cells were fixed in 4% formaldehyde PBS solution for 30 min at room temperature, treated with PBS that contained 50 mM NH_4Cl for 10 min, and then washed twice in PBS. Cells were permeabilized in PBS 0.1% Triton X 100 for 5 min and washed twice with PBS. Coverslips were treated with 1 ml of anti-PC2 Nter M antibody (50 μg) solution that contained 0.2% gelatin at room temperature for 2 h. After three washes with PBS, cells were treated with a PBS 0.2% gelatin solution that contained a secondary anti-rabbit rhodamine-conjugated antibody (Santa Cruz [DBA], Milano, Italy) at room temperature in dark condition for 1 h. After three washes in PBS, cells were analyzed by a Zeiss Axiovert 200 fluorescence microscope equipped with a back-illuminated CCD camera (Roper Scientific, Tucson, AZ), excitation and emission filter wheels (Sutter Instrument Company, Novato, CA), and piezoelectric motoring of the z stage (Physik Instrumente, GmbH and Co., Karlsruhe, Germany). In some experiments, the anti-N-term anti-PC2 antibody was added to the pipette solution and, after whole cell configuration was reached, a series of ramps protocols were applied at a rate of 0.1/s, the first one to be used as internal control.

Electrophysiology

Cell plates were transferred into a recording chamber and secured to an upright Olympus microscope. Cells were perfused with standard saline that contained (in mM) 152 NaCl, 2.5 KCl, 2 CaCl_2 , 1 MgCl_2 , and 5 HEPES free acid. The pH was adjusted to 7.4 with NaOH for all bath solutions. Osmolality was adjusted to 305 mOsm/kg with sucrose. Standard pipette solution contained (in mM) 120 KCl, 10 NaCl, 2 MgCl_2 , 0.5 CaCl_2 , 5 EGTA, 10 HEPES, and 2 ATPMg. The pH and the osmolality were adjusted to 7.2 with KOH and to 310 mOsm/kg with

sucrose, respectively. When filled with intracellular solution, the pipette resistance in the bath was in the range of 5 to 6 M Ω .

All chemicals were purchased from Sigma Aldrich (St. Louis, MO) except tetrodotoxin (TTX), charibdotoxin (ChTx), and paxilline (Alomone Labs, Jerusalem, Israel).

Electrical recordings were performed by an Axopatch 200B patch-clamp amplifier (Axon Instruments, Inc., Union City, CA). Seal resistance was always $>3\text{ G}\Omega$. Series resistance was routinely compensated at 80%. Membrane currents were sampled at 10 kHz after filtering at the corresponding Nyquist frequency by a four-pole Bessel filter and were acquired on a PC-486 computer with 12-bit A/D-D/A Digidata 1200B converter (Axon Instruments). Voltage protocol generation and data acquisition were performed using pClamp versions 7.0.1 (Axon Instruments). Correction for liquid-junction potentials was applied directly to the holding potential (15). To avoid electrical coupling among cells as a result of gap junctions, only isolated cells were recorded.

Results are given as mean \pm SEM and examined by nonparametric statistical tests. $P < 0.05$ was considered statistically significant.

Results

General Observations

In native HEK-293 cells, depolarizing commands from a holding potential of -120 mV in voltage-clamp whole-cell configuration evoked a large outward current ($7.25\text{ pA/pF} \pm 1.03$; $n = 40$) and a much smaller inward current ($-2.35 \pm 0.02\text{ pA/pF}$; $n = 106$; Figure 1a). The overall excitability profile

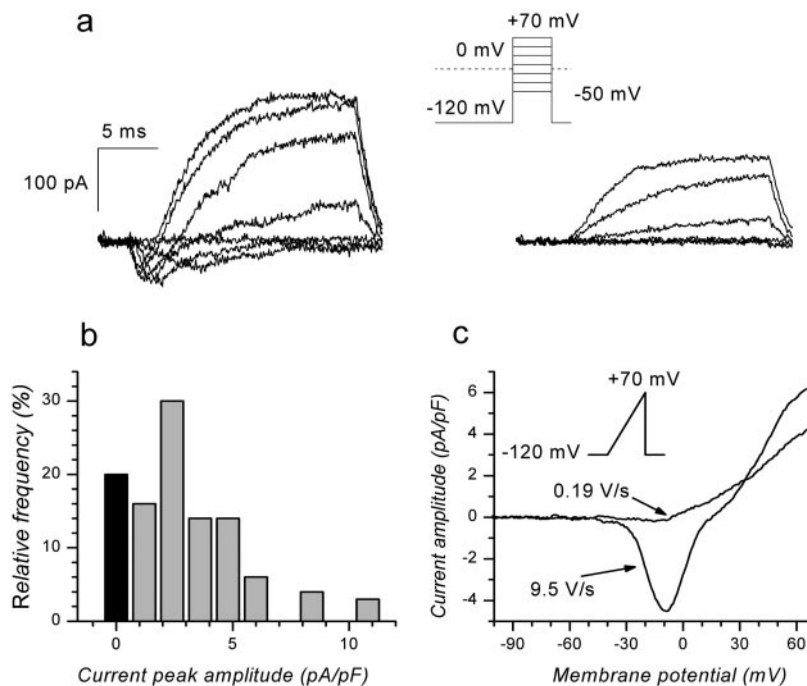


Figure 1. Current pattern in native HEK-293 cells. (a) Voltage-clamp recordings from a typical native HEK-293 cell stimulated with protocols shown in the inset. Depolarization to potentials from -50 to 70 mV in 20-mV steps were preceded by a 200 ms of preconditioning pulse at -120 mV (left traces, protocol; solid line) or 0 mV (right traces, protocol; dotted line). More positive holding potentials cause, besides a voltage-dependent inactivation of the inward current, a reduction in the outward one. Current traces are plotted in terms of current density (pA/pF) to normalize the total current to cell area. The mean cell membrane capacitance was $25.8 \pm 2.32\text{ pF}$ ($n = 40$). Between trials, holding potential was kept at the resting potential of the cell ($27.1 \pm 2.8\text{ mV}$). Leak currents were subtracted online. (b) Inward current peak amplitude distribution. ■, Failures in nonspecific cation current (I_{CC}) observation. (c) Instantaneous I-V relationship obtained by means of a ramp protocol, as shown in the inset. Leak currents were subtracted offline. Comparison of different ramp steepness: 9.5 V/s or 0.19 V/s .

strongly depended on the holding potential: The small inward current developed to full size only when a preconditioning pulse at a negative potentials was applied (-120 mV in Figure 1a, left) but disappeared when the holding potential was 0 mV (Figure 1a, right). The last experimental condition also reduced the outward current amplitude (mean decrement $62.6 \pm 11.8\%$; $n = 7$; Figure 1a).

The inward current was observed in 81.1% of cells ($n = 106$). Inward current peak amplitude was variable, and its distribution was skewed to the right (Figure 1b). No significant differences were observed in different cell batches. When ramp protocols were used instead of square pulses, the inward current was observed only when the ramp slope was sufficiently steep (Figure 1c).

Ionic and Pharmacologic Properties of the Inward Current

We first tried to identify the ionic basis of the inward current. To determine the reversal potential (E_{rev}), the inward current was evoked by a depolarizing step at 0 mV from a holding potential of -120 mV. At the current peak, the membrane was instantly repolarized to potentials ranging from -20 to 80 mV (Figure 2a, inset). The tail current amplitude allowed determination of the instantaneous I–V relationship, with a reversal potential of 47.6 mV (Figure 2a). This value was not coincident with the equilibrium potential of any of the ions present in standard saline and was 12.6 mV more negative than E_{Na} (-60.2 mV).

The channel permeability to cations was tested by substituting external Na^+ with equimolar amount of different monovalents: Substitution of external Na^+ with N-methyl-D-glucamine (NMDG; Figure 2b), an impermeant cation, reversed inward current. Conversely, no differences in the outward current were observed. The reversed current was not due to an efflux of internal Na^+ , as it was also observed when this ion was substituted with NMDG in the internal solution (data not shown). The rank order of monovalent permeability, as deduced from peak current amplitudes, was $Na^+ > Li^+ > NH_4^+ > K^+ > Rb^+$ (Figure 2c). Substitution of Na^+ with Cs^+ induced a suppression of the inward current. When all of the external NaCl was substituted with KCl and monovalents in pipette solution were replaced by an equimolar amount of NMDG (Figure 2d), it was still possible to observe the inward current, albeit lower than in control ($31.75 \pm 0.04\%$; $n = 6$).

The inward current was insensitive to blockers of chloride channels ($200 \mu\text{M}$ anthracene-9-carboxylic acid [9-AC] and $100 \mu\text{M}$ niflumic acid), of voltage-gated Na channels ($1 \mu\text{M}$ TTX) and K^+ channels (30 mM TEA) and of L-type Ca^{2+} channel ($100 \mu\text{M}$ nifedipine). The current was also unaffected by application of P-receptor antagonist ($100 \mu\text{M}$ suramine), of membrane-permeant cyclic nucleotide analogs ($100 \mu\text{M}$ 8-Br-cGMP and 8-Br-cAMP), of Ca^{2+} entry channel inhibitor $25 \mu\text{M}$ 2-aminoethoxydiphenylborane (APB), and of ENaC channel blocker $1 \mu\text{M}$ amiloride (Figure 2e). In standard experimental condition, E_{Cl} was near 0 mV. Consistent with insensitivity to 9-AC and niflumate, changes in external $[Cl^-]$ (data not shown) did not modify inward current amplitude. Conversely, this current was significantly reduced (Figure 2e) by application of nonselective

cation channels blockers (16,17) such as $100 \mu\text{M}$ Cd^{2+} , $100 \mu\text{M}$ Ni^{2+} , 1 mM Gd^{3+} , 1 mM La^{3+} , $100 \mu\text{M}$ SKF96365, and higher concentrations of amiloride (100 , 200 , and $500 \mu\text{M}$).

In cells that were perfused with 0 Ca^{2+} -EGTA saline (Figure 2f), the current peak amplitude decreased by $12.4 \pm 4.55\%$ ($n = 6$; $P < 0.05$). It is noteworthy that, besides this effect on the peak inward current amplitude, a reduction in the outward current was also observed ($54.1 \pm 12.9\%$; $n = 6$; $P < 0.05$). Substitution of external Ca^{2+} with 4 mM Ba^{2+} (Figure 2g) ensued to a slight increase in the inward current ($13.8 \pm 2.07\%$; $n = 5$; $P < 0.05$) and to a large decrease in the outward current ($73.3 \pm 10.6\%$; $n = 5$; $P < 0.05$). Because of its ionic and pharmacologic properties, the inward current hereafter is indicated as nonspecific cationic current (I_{CC}).

Kinetic Properties of I_{CC}

Although the maximal current amplitude was variable from cell to cell, its ionic composition, as well as kinetic and pharmacologic properties, was identical in all cells examined. To improve the accuracy of the study, we performed kinetic analysis in a group of 10 cells that showed currents larger than -100 pA. Interference by the larger outward current was prevented by application of TEA 30 mM.

The I–V relationship was obtained by applying 20 ms of depolarizing pulses ranging from -80 mV to 60 mV, in 20 -mV increments, from a holding potential of -120 mV, to completely remove voltage-dependent inactivation (Figure 3a, inset). The inward current could be evoked at potentials that were more positive than -50 mV and peaked at -10 mV (Figure 3a). Cells were conditioned for 300 ms to different holding potentials and then depolarized to 0 mV (Figure 3b, inset). This allowed us to determine the steady-state inactivation curve (Figure 3c, ∇). To determine the steady-state activation curve (Figure 3c, Δ) the peak current was divided by the driving force and then normalized with respect to maximum value. The inward current inactivated rapidly, with an average time constant of 1.1 ± 0.12 ms at 0 mV ($n = 10$), whereas the removal of inactivation, studied with a conventional double-pulse protocol, was a much slower process ($\tau = 43.5 \pm 0.95$ ms; $n = 6$; Figure 3d).

Outward Current

The outward current was completely blocked by perfusion with TEA 30 mM saline (Figure 4a) and was insensitive to Cl^- channel blockers (Figure 4b). It therefore was identified as a K^+ current (I_K).

In the presence of 100 nM ChTx and paxilline (Figure 4b), two selective blockers of BK-type Ca^{2+} -activated voltage-dependent K^+ channels (18,19), the total I_K was decreased to $55.0 \pm 17.3\%$ (ChTx, $n = 3$) and to $48.5 \pm 15.4\%$ (paxilline, $n = 3$). Conversely, $100 \mu\text{M}$ apamine, a selective blocker of SK-type Ca^{2+} -dependent K^+ channels (20), and $100 \mu\text{M}$ nifedipine, an L-type Ca_v -channel blocker, were ineffective (Figure 4b). The paxilline-insensitive component of I_K was similar in extent to that observed after inactivation of I_{CC} by means of a slower ramp protocol (Figure 4c).

All drugs that blocked I_{CC} ensued also in a partial decrease of I_K . In particular (Figure 4d), the progressive block of I_{CC} that

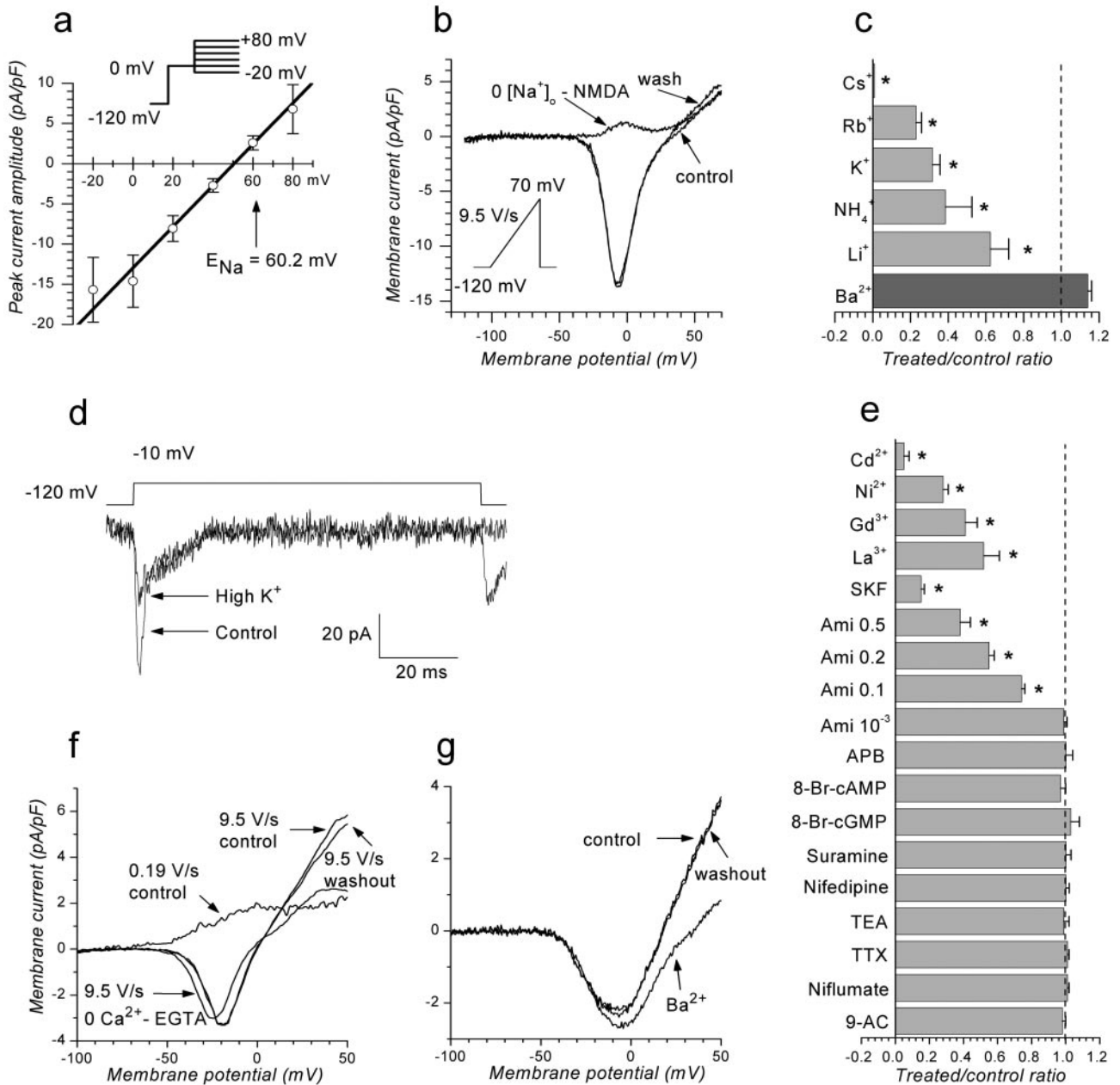


Figure 2. Ionic and pharmacologic properties of I_{CC} . (a) I_{CC} reversal potential (E_{rev}) calculated as the zero current point, from linear regression to the instantaneous I–V relationship, obtained by means of the protocol shown in the inset. Data were obtained in 30 mM TEA. Arrow indicates Na^+ equilibrium potential, as calculated from Nernst. (b) Instantaneous I–V relationship obtained by the ramp protocol shown in the inset. Traces were recorded in control solution, in N-methyl-D-glucamine (NMDG)-saline, and back in control (wash). In NMDG-saline, all external Na^+ was replaced with equimolar amounts of NMDG. (c) Effect of equimolar substitution of external Na^+ with different monovalents (light gray columns) or substitution of external Ca^{2+} (dark gray column) with 4 mM Ba^{2+} . The effects were calculated as the ratio between inward current peak amplitude before and after the treatments. Vertical dashed line indicates control level. Substitutions with Li^+ , NH_4^+ , Rb^+ , and Cs^+ were performed on the same set of cells ($P < 0.001$, $n = 6$). Data on K^+ permeability were obtained in a high external $[K^+]$ solution, which contained 152 mM KCl and 0 mM NaCl, by means of the protocol shown in d. For reversing K^+ gradient, all NaCl and KCl in the pipette solution were substituted with NMDG. (d) Traces evoked by a single depolarizing step from -120 to -10 mV (inset) in control and high external K^+ solution. Pipette was filled with (in mM) 120 NMDG, 20 TEA-Cl, 0 NaCl, 0 KCl, 0.5 $CaCl_2$, and 2 $MgCl_2$. In the presence of a reversed K^+ gradient and in the absence of Na^+ , an inward current was still present, although reduced in amplitude. (e) Pharmacologic sensitivity of I_{CC} to several drug applications (see text) ($n = 6$). The effects were calculated as the ratio between peak amplitude before and after treatments. Vertical dashed line indicates control level. (f) I–V relationship obtained by a fast (9.5 V/s) ramp protocol in control solution, in 0 Ca^{2+} /10 mM EGTA saline, and back in control. EGTA saline was obtained by replacing an equimolar amount of NaCl with 10 mM EGTA and adding no Ca^{2+} . Residual K^+ current (I_K) in EGTA saline was lower than control but similar in extent to the one recorded, in the same cell, when I_{CC} was completely inactivated by a slower ramp protocol (0.19 V/s). (g) I–V relationship obtained by a fast ramp protocol (9.5 V/s) in control solution, after substitution of extracellular Ca^{2+} with 4 mM Ba^{2+} , and back in control.

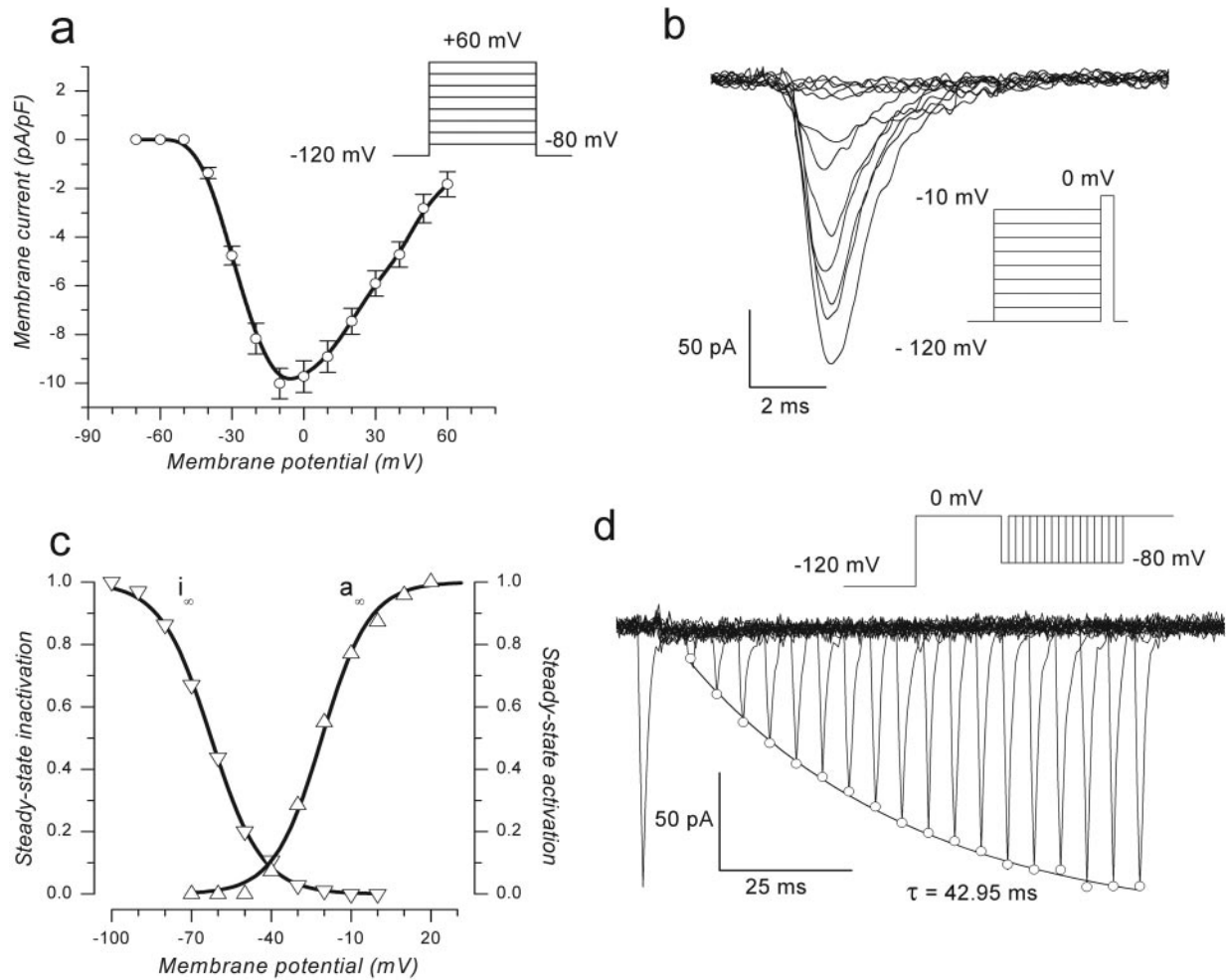


Figure 3. Voltage dependence of I_{CC} . (a) Average I–V relationship obtained in TEA saline in 10 sample cells, by the protocol shown in the inset. (b) Development of inactivation. Family of tracings obtained in one representative cell in response to the protocol shown in the inset. (c) Steady-state activation curve, a_{∞} (Δ). The experimental points (average of 10 cells) were fitted by the Boltzmann equation $a_{\infty} = 1/[1 + \exp\{(V_0 - V)/k\}]$, where the half activation voltage, V_0 , was equal to -20.5 mV and the slope factor, k , is equal to 9.45 mV. The steady-state inactivation curve, $i_{\infty}(V)$ (∇ , average of six cells) was fitted by the Boltzmann equation: $i_{\infty} = 1/[1 + \exp\{(V - V_0)/k\}]$, where $V_0 = -62.6$ mV and $k = 9.48$ mV. (d) Time course of removal of inactivation at -80 mV. Family of tracings obtained by a double pulse protocol (inset), consisting of two subsequent steps to 0 mV, the first from a holding potential of -120 mV and the second after a variable time at -80 mV. The peak amplitude of the current evoked by the second pulse increased exponentially with time ($t = 43.5 \pm 0.95$ ms; $n = 6$; solid line) as a result of an increasing percentage of channels recovered from inactivation.

was induced by increasing concentrations of amiloride led to a proportional reduction in I_K .

Molecular Biology Experiments

Because many, although not all, of the properties of this channel activity were similar to those of PC2, whose presence at endoplasmic reticulum and plasma membrane in native HEK-293 cells has already been reported (14) and shown in Figure 5a, we tested whether the I_{CC} could be mediated by these channels. For assessment of this hypothesis, PC2 expression was inhibited by siRNA-mediated suppression. Figure 5a shows representative current traces from a control (upper), a WTPC2⁻ (center), and a WTPC2⁻/FLPC2 cell (lower), respectively. In WTPC2⁻ cells, the current decreased in amplitude and was

completely absent in a higher number of cells (37.5 versus 18.9%). The I_{CC} mean peak amplitude was significantly lower than in native control cells (-1.08 ± 0.36 pA/pF versus -2.54 ± 0.23 pA/pF; $n = 20$; $P < 0.05$; Figure 5b), suggesting that I_{CC} is associated with, if not indeed sustained by, PC2 expression. To assess whether the decrease of I_{CC} in silenced cells was specifically due to PC2 expression inhibition, we tested whether transient transfection with GFP-tagged heterologous PC2 could restore the current. Cells in which the transient transfection was able to escape silencing were identified by the green fluorescence. These cells did show a positive staining at plasma membrane level (Figure 5b), indicating that, despite the presence of PKD2 siRNA, the exogenously overexpressed PKD2 RNA did likely overcome the “nontotal” efficiency of the siRNA. This

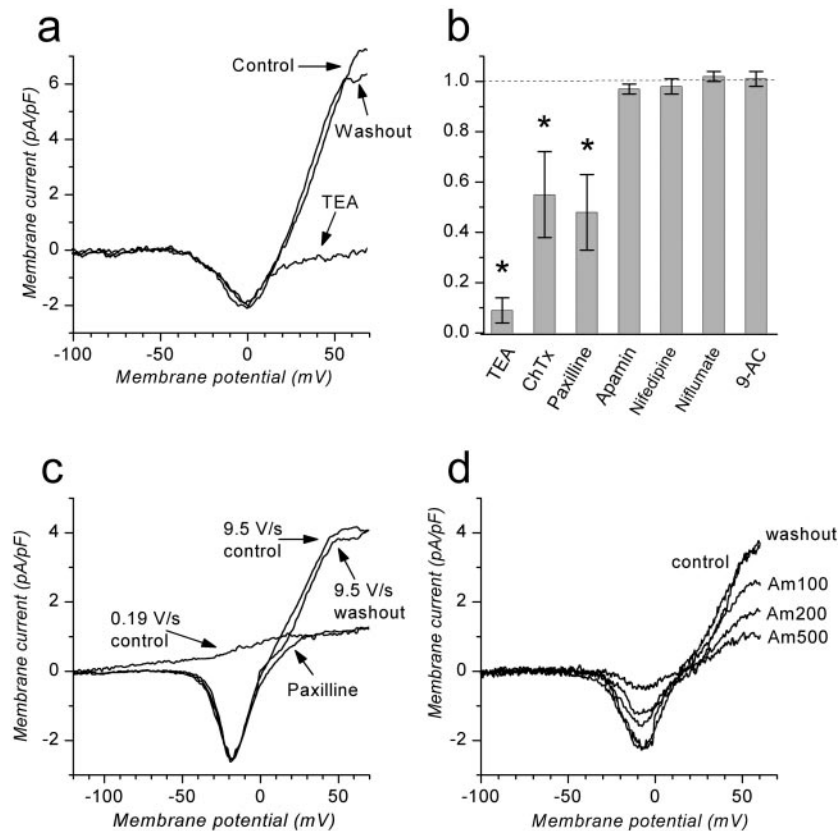


Figure 4. Presence of a calcium-activated component in I_K . (a) Mean I–V relationship obtained in six sample cells by a fast ramp protocol (9.5 V/s). Traces were obtained in control solution, in TEA-saline, and back in control (washout). In TEA-saline, equimolar amounts of NaCl were replaced by 30 mM TEA. (b) Pharmacologic sensitivity of I_K . The effects were calculated as the ratio between peak amplitude before and after treatments. Horizontal dotted line indicates control level. (c) I–V relationship obtained in control solution in the presence of paxilline, and back in control, obtained by means of a fast ramp protocol (9.5 V/s). Once again, the paxilline-insensitive component of I_K was similar in extent to that recorded, in the same cell, after I_{CC} had completely been inactivated by a slower ramp protocol (0.19 V/s). (d) Application of amiloride in a cell that was stimulated by the same protocol of a. A proportional reduction in both inward and outward currents was evident at increasing the concentration of the drug.

was consistent with the slight immunoblot detection of endogenous PC2 in WTPC2⁻ siRNA-suppressed cells (Figure 5a, inset). When WTPC2⁻ cells were transiently transfected with heterologous PC2 (WTPC2⁻/FLPC2), I_{CC} peak amplitude recovered to a higher value than control (-4.48 ± 0.32 pA/pF; $P < 0.05$; $n = 16$), whereas transient transfection with a PC2 that lacked the PC1 interacting region (WTPC2⁻/PC2stop) was ineffective (-1.19 ± 0.58 ; $n = 16$). In WTPC2⁻ cells, I_K was also reduced (4.32 ± 0.90 versus 7.28 ± 1.26 pA/pF; $n = 16$; $P < 0.5$), and this effect was rescued in WTPC2⁻/FLPC2 cells (14.5 ± 1.14 pA/pF; $n = 16$; $P < 0.5$) but not in WTPC2⁻/PC2stop cells (4.17 ± 0.78 pA/pF; $n = 16$; Figure 5b).

Consistently, as shown in Figure 5c, intracellular perfusion with an anti-PC2 antibody (anti-N-terM) (13,14), targeting the PC2 N-terminal region, almost completely abolished the inward current (0.22 ± 0.12 pA/pF) with respect to control (2.89 ± 0.21 pA/pF; $n = 16$). The full effect developed in approximately 2 min ($n = 16$; mean time 2 hr 20 min \pm 20 min) after the whole-cell configuration was obtained. As control, currents that were recorded in cells that were perfused with anti-Ig antibody remained unaffected up to 45 min.

Because PC2 channels are known to be modulated by PC1, we analyzed the I_{CC} current evoked in cells that were transfected with PC1 cytoplasmic tail anchored to the plasma membrane *via* the transmembrane domain of Trk-A (HEK^{TrkPC1}) (13,21). As shown in Figure 5d, recordings that were obtained in HEK^{TrkPC1} cells' I_{CC} were qualitatively similar to but higher than those that were obtained in native HEK-293 (-4.6 ± 0.05 versus -2.35 ± 0.02 pA/pF; $n = 106$; $P < 0.05$), whereas in HEK^{Trk0} cells, expressing membrane Trk-A regions only, current amplitude was similar to that of native cells (-2.27 ± 0.65 versus -2.41 ± 0.13 pA/pF; $n = 16$; $P > 0.5$; Figure 5e). In particular, the steady-state activation and inactivation curves and the normalized I–V relationship were virtually identical (data not shown). The number of cells in which I_{CC} was absent was much greater in control HEK^{Trk0} cells (19.9 versus 5.7%), whereas the percentage of cells that displayed medium (5 to 10 pA/pF) or large (>10 pA/pF) peak currents were much higher in HEK^{TrkPC1} cells (32.0 versus 10.4; $n = 106$). Also, total I_K was larger in HEK^{TRKPC1} cells, but this increase was NS (7.54 ± 1.06 in control versus 9.05 ± 1.029 pA/pF in transfected cells; $n = 40$; $P > 0.5$; data not shown). Immunofluorescence analysis on

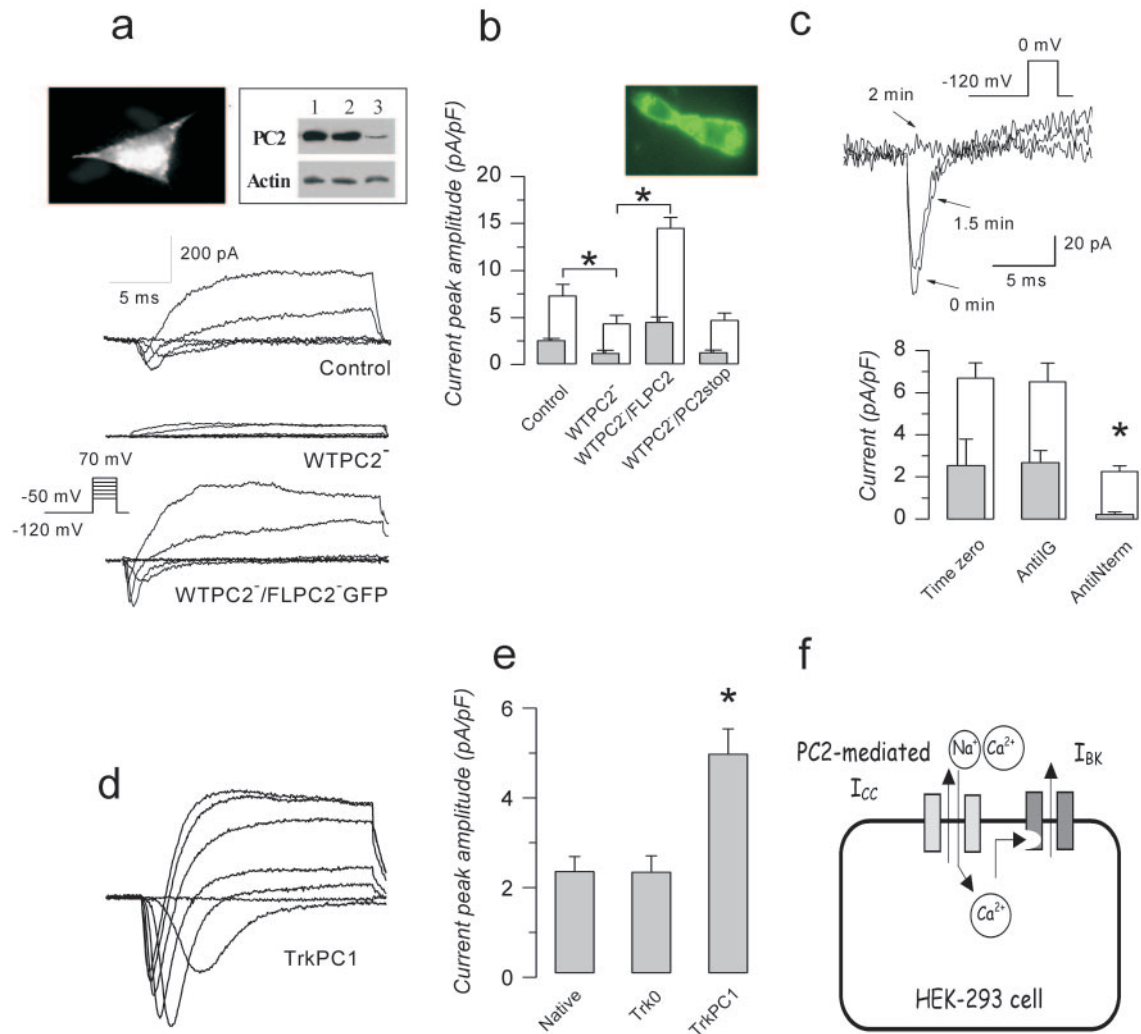


Figure 5. Effect of modification of PC2 and PC1 expression on current amplitude. (a) Voltage-clamp recordings, obtained by means of the indicated protocol, from a control HEK^{PSuper} cell (upper trace, $C_m = 21$ pF), a WTPC2⁻ (center trace, $C_m = 19$ pF), and a WTPC2⁻ cell transiently transfected with full-length heterologous GFP-tagged PC2 (lower trace, WTPC2⁻/FLPC2, $C_m = 24$ pF). (Inset, left) Immunofluorescence analysis of PC2 in native HEK-293 cells. (Inset, right) Western blot analysis of PC2 in HEK^{PSuper} cells (lane 1), in HEK^{PSuperCS} cells stably transfected with the siRNA expressing a PKD2-unrelated sequence (lane 2), and in WTPC2⁻ cells (lane 3). Approximately 20 μ g of total cell extracts were analyzed by Western blotting and probed with anti-N-terM PC2 (PC2) and with anti- β -actin (actin). (b) Mean peak amplitude of I_{CC} (■) and of total I_K (□) measured in control cells ($n = 20$), WTPC2⁻ cells ($n = 20$), WTPC2⁻/FLPC2 ($n = 16$), and WTPC2⁻ cells overexpressing the truncated PC2 (WTPC2⁻/PC2stop; $n = 16$). (Inset) Fluorescence analysis of WTPC2⁻/FLPC2-GFP cells showed staining of both endoplasmic reticulum and plasma membrane. (c) Intracellular perfusion with an anti-N-terM PC2 and an anti-Ig antibody. Antibodies (150 μ g/ml) were added to the pipette solution, and after whole-cell configuration was reached, a series of ramps protocols were applied, at a rate of 0.1/s, the first one to be used as internal control. (Top) Currents evoked by a single depolarizing step to 0 mV, from a preconditioning level of -120 mV (inset). Three traces, recorded immediately, after 1.5 min, and after 2 min after cell membrane rupture, are superimposed. (Bottom) Mean peak amplitude of I_{CC} (■) and of total I_K (□) measured immediately after whole-cell configuration was obtained (time zero, left, $n = 32$), after at least 3 min of perfusion with the anti-N-terM PC2 (center; $n = 16$) or an anti-Ig antibody (right; $n = 16$). (d) Voltage-clamp recordings, obtained by the protocol shown in a, from a TrkPC1 cell overexpressing the PC1 tail (14,21), with $C_m = 23$ pF. (e) Mean peak amplitude of I_{CC} measured in a set of native cells ($n = 106$), in Trk0 cells (14,21) lacking the PC1 sequence ($n = 32$), and in TrkPC1 cells ($n = 106$). (f) Schematic drawing of a possible functional co-localization of I_{CC} and $I_{K(Ca)}$ (see Discussion for further details).

native and full-length PC2 transfected cells (Figure 5, g and h, respectively) by primary anti-N-terM and secondary rhodamine-conjugated antibody further confirm the presence of PC2 at plasma membrane level.

Discussion

Here we present the first functional evidence for a native I_{CC} not previously described in HEK-293 cells and highly associated with PC2, that is expressed on cell plasma membrane (14).

The subcellular localization of PC2 has been a subject of debate. Although different works suggest that PC2 is an endoplasmic reticulum resident protein (8,22), other evidence (23,24) supports its functional presence on the plasma membrane. It has indeed been demonstrated (25) that PC1 and PC2 co-distribute in primary cilia of kidney epithelium, most likely playing a critical role in the mechano-transduction pathway that allows fluid flow sensitivity.

HEK-293 cells are a widely used expression system for ion channel studies, although they are provided by a complex set of endogenous currents. Despite many observations of a TEA-sensitive delayed rectifier K^+ current, not all authors agree about the presence of native chloride conductances (26,27). A voltage-dependent Ca^{2+} current, sensitive to dihydropyridine but different from L-type, has been described (28). Occasionally, findings of a voltage-dependent TTX-sensitive Na^+ current have also been reported (29), although HEK-293 cells endogenously express the auxiliary $\beta 1A$ -subunit of voltage-gated sodium channel but not the pore-forming α one (30). In addition, a nonspecific cation channel (31) has been described. Recordings of an ultraviolet light-induced nonselective cation current (32) and functional expression of a proton-gated channel (33) and of several members of the TRPC channel family (34,35) also contribute to this complex picture. The lack of previous observations of I_{CC} and I_{KCa} in HEK-293 cells is not surprising given the large negative holding potential that is necessary to avoid I_{CC} inactivation and to the tight functional link between the two.

As concerns I_{CC} identification, the decrease in its peak amplitude after either PC2 selective silencing or perfusion with the anti-PC2 antibody indicates that it is highly associated with, if not sustained by, PC2. Nevertheless, some features of the native current here described do not perfectly match those of PC2. In particular, depending on the cell system, PC2 has been reported to be more or equally permeant to K^+ in respect to Na^+ (36), whereas here we report a higher Na^+ selectivity with respect to K^+ (3:1). This discrepancy does not necessarily rule out that I_{CC} can be mediated by PC2. It has been reported that different expression systems, in the case of channel reconstitution, or tissue specificity, in the case of native channel activity (25,37), can modify biophysical channel properties, as a result of co-assembly with different subunits or to specific posttranscriptional processing. In particular, hetero-oligomerization among PC2 and TRPC channels has been described (38). This observation may be important considering that, as previously mentioned, several members of the TRPC family, as well as voltage-gated channels, are expressed in native HEK-293 cells. If such a hetero-oligomerization takes place in native HEK-293, regarding TRPC or other endogenous channel subunits, then this could account for functional changes of the purported native PC2 channel.

Although we were unable to detect any Ca^{2+} influx, we found a decrease in I_{CC} in the absence of external Ca^{2+} and an increase after substitution of external Ca^{2+} with Ba^{2+} . Moreover, we provided independent and consistent evidences that a Ca^{2+} influx through I_{CC} is required to trigger an $I_{K(Ca)}$, thus allowing us to use the latter as a biosensor for Ca^{2+} influx:

When I_{CC} was inactivated by preconditioning the membrane at -50 mV or by means of a slow voltage ramp (0.19 V/s), the amplitude in I_K was also decreased. Consistently, all drugs that blocked I_{CC} ensued also in a partial decrease of I_K that was instead unaffected when cells were perfused with NMDG-saline or for extracellular Na^+ substitution with different monovalents, despite the great I_{CC} amplitude reduction caused by these treatments. In the absence of extracellular Ca^{2+} , I_K was reduced and the residual component was comparable with that observed after inactivation of I_{CC} by preconditioning at -50 mV. In 4 mM Ba^{2+} , which is known not to activate $I_{K(Ca)}$ (18), I_K was reduced, despite the light increase in I_{CC} peak amplitude. Furthermore, I_K amplitude was lowered by PC2 silencing and by anti-PC2 perfusion.

Taken together, all data strongly suggest a functional coupling between I_{CC} and a fraction of I_K , by means of an ionic flux different from monovalents, most likely an external Ca^{2+} influx. This suggests that the I_K here described is, in fact, the sum of a classical delayed rectifier current and of a Ca^{2+} -dependent K^+ current, $I_{K(Ca)}$. The sensitivity of this current to ChTx and paxilline but not to Apamine further confirms its identification as a BK-type $I_{K(Ca)}$.

It is interesting that I_{CC} is enhanced, without changes in its properties, by overexpression of the PC1 tail that contained the PC2 interacting domain. This is in agreement with former findings that expression of TrkPC1 peptide increases the ATP- and serum-evoked cytosolic Ca^{2+} concentration (13,14). The ATP-evoked increase has a biphasic pattern with a peak as a result of the release from intracellular stores and a plateau as a result of the Ca^{2+} influx through cationic Ca^{2+} -permeable plasma channels. The last component may be sustained by the current described here.

Increasing evidence suggests that a functional co-localization of Ca^{2+} -activated K channels and Ca^{2+} channels could occur, thus leading to specific effects by local increase in intracellular Ca^{2+} (39–41). If this were the case in HEK-293 cells, as schematically drawn in Figure 5f, then this may explain how even a small calcium influx through I_{CC} could be effective in activating $I_{K(Ca)}$. Because PC1 seems to be required for recruitment of PC2 to the plasma membrane (23), the heterologously expressed PC1 could translocate to it additional PC2 molecules, thus increasing the current.

As concerns pharmacologic profile of I_{CC} , although qualitatively consistent with PC2 sensitivity (9,10,36,42), it must be noted that amiloride, La^{3+} , Gd^{3+} , and Ni^{2+} lack specificity, blocking various channels and transporters. The dose-response relation of the effect of amiloride on I_{CC} (data not shown) gave a half-maximum inhibition at 245 μM , slightly higher than that reported for native PC2 (36). Significantly, values much similar to ours were observed in native PC2 from rat left ventricular myocytes (130 μM) (42), and it must be considered that even in the same experimental model, drug sensitivity could significantly differ when estimated by whole-cell or single-channel recording (43). We also reported sensitivity to Cd^{2+} and to SKF96365, a Ca^{2+} entry blocker that inhibits also nonselective channels in endothelial cells (16).

Although many studies report no voltage dependence of PC2

(10,23,36), our data are consistent with the reported increase of P_o with negative potentials (7–9,11). Changes in PC2 expression by either endogenous or heterologous PC2, as well as heterologous PC1 expression and cell perfusion with anti-PC2 antibody, do affect I_{CC} , suggesting that it could be sustained by PC2. Nevertheless, the ionic permeability and the pharmacologic sensitivity of I_{CC} do not perfectly match those of PC2, as reported in the literature. As a consequence, a much more indirect association between I_{CC} and PC2 cannot be excluded. A biophysical characterization by means of single-channel patch-clamp technique will be of great interest to assess these two different predictions.

If our hypothesis is confirmed, then HEK-293 cells could be regarded as a suitable and readily accessible tool to study PC1 and PC2 macromolecular interactions, thus contributing to the elucidation of physiopathologic mechanisms of ADPKD.

Acknowledgments

We gratefully acknowledge Dr. Mascia Benedusi and Dr. Lucia Cadeddi for participating in some initial recordings, Dr. Erika Franzoni for technical assistance, and Dr. Elisabeth Jankins for reading of the manuscript in English. This work was supported by grants from MURST, CaRiFe, and Telethon (E1250).

Preliminary data were presented at the EMBO meeting, Capri, September 20 to 23, 2004; and at the XVIII SIBPA meeting, Pisa, Italy, September 23 to 25, 2004.

References

- Gabow PA, Grantham J: Polycystic kidney disease. In: *Diseases of the Kidney*, 6th Ed., edited by Schrier RW, Gottschalk CW, Boston, Little, Brown & Co, 1997, pp 521–560
- The polycystic kidney disease 1 gene encodes a 14 kb transcript and lies within a duplicated region on chromosome 16. The European Polycystic Kidney Disease Consortium. *Cell* 77: 881–894, 1994
- Polycystic kidney disease: The complete structure of the PKD1 gene and its protein. The International Polycystic Kidney Disease Consortium. *Cell* 81:289–298, 1995
- Hughes J, Ward CJ, Peral B, Aspinwall R, Clark K, San Millan JL, Gamble V, Harris PC: The polycystic kidney disease 1 (PKD1) gene encodes a novel protein with multiple cell recognition domains. *Nat Genet* 10: 151–160, 1995
- Lakkis M, Zhou J: Molecular complexes formed with polycystins. *Nephron Exp Nephrol* 93: e3–e8, 2003
- Vassilev PM, Guo L, Chen XZ, Segal Y, Peng JB, Basora N, Babakhanlou H, Cruger G, Kanazirska M, Ye C, Brown EM, Hediger MA, Zhou J: Polycystin-2 is a novel cation channel implicated in defective intracellular Ca^{2+} homeostasis in polycystic kidney disease. *Biochem Biophys Res Commun* 282: 341–350, 2001
- Gonzalez-Perrett S, Batelli M, Kim K, Essafi M, Timpanaro G, Moltabetti N, Reisin IL, Arnaout MA, Cantiello HF: Voltage dependence and pH regulation of human polycystin-2-mediated cation channel activity. *J Biol Chem* 277: 24959–24966, 2002
- Koulen P, Cai Y, Geng L, Maeda Y, Nishimura S, Witzgall R, Ehrlich BE, Somlo S: Polycystin-2 is an intracellular calcium release channel. *Nat Cell Biol* 4: 191–197, 2002
- Xu GM, Gonzalez-Perrett S, Essafi M, Timpanaro GA, Montalbetti N, Arnaout MA, Cantiello HF: Polycystin-1 activates and stabilizes the polycystin-2 channel. *J Biol Chem* 278: 1457–1462, 2003
- Chen XZ, Vassilev PM, Basora N, Peng JB, Nomura H, Segal Y, Brown EM, Reeders ST, Hediger MA, Zhou J: Polycystin-L is a calcium-regulated cation channel permeable to calcium ions. *Nature* 401: 383–386, 1999
- Liu Y, Li Q, Tan M, Zhang YY, Karpinski E, Zhou J, Chen XZ: Modulation of the human polycystin-L channel by voltage and divalent cations. *FEBS Lett* 525: 71–76, 2002
- Mochizuki T, Wu G, Hayashi T, Xenophontos SL, Veldhuisen B, Saris JJ, Reynolds DM, Cai Y, Gabow PA, Pierides A, Kimberling WJ, Breuning MH, Deltas CC, Peters DJ, Somlo S: PKD2, a gene for polycystic kidney disease that encodes an integral membrane protein. *Science* 272: 1339–1342, 1996
- Aguiari G, Banzi M, Gessi S, Cai Y, Zeggio E, Manzati E, Piva R, Lambertini E, Ferrari L, Peters DJ, Lanza F, Harris PC, Borea PA, Somlo S, Del Senno L: Deficiency of polycystin-2 reduces Ca^{2+} channel activity and cell proliferation in ADPKD lymphoblastoid cells. *FASEB J* 18: 884–886, 2004
- Aguiari G, Campanella M, Manzati E, Pinton P, Banzi M, Moretti S, Piva R, Rizzuto R, Del Senno L: Expression of polycystin-1 C-terminal fragment enhances the ATP-induced Ca^{2+} release in human kidney cells. *Biochem Biophys Res Commun* 301: 657–664, 2003
- Neher E: Correction for liquid junction potentials in patch clamp experiments. *Methods Enzymol* 207: 123–131, 1992
- Nilius B, Viana F, Droogmans G: Ion channels in vascular endothelium. *Annu Rev Physiol* 59: 145–170, 1997
- Inoue R, Okada T, Onoue H, Hara Y, Shimizu S, Naitoh S, Ito Y, Mori Y: The transient receptor potential protein homologue TRP6 is the essential component of vascular $\alpha(1)$ -adrenoceptor-activated Ca^{2+} -permeable cation channel. *Circ Res* 88: 325–332, 2001
- Sun XP, Schlichter LC, Stanley EF: Single-channel properties of BK-type calcium-activated potassium channels at a cholinergic presynaptic nerve terminal. *J Physiol* 518: 639–651, 1999
- Miller C, Moczydlowski E, Latorre R, Phillips M: Charybdotoxin, a protein inhibitor of single Ca^{2+} -activated K^{+} channels from mammalian skeletal muscle. *Nature* 313: 316–318, 1985
- Hu H, Shao LR, Chavoshy S, Gu N, Trieb M, Behrens R, Laake P, Pongs O, Knaus HG, Ottersen OP, Storm JF: Presynaptic Ca^{2+} -activated K^{+} channels in glutamatergic hippocampal terminals and their role in spike repolarization and regulation of transmitter release. *J Neurosci* 21: 9585–9597, 2001
- Manzati E, Aguiari G, Banzi M, Manzati M, Selvatici R, Falzarano S, Maestri I, Pinton P, Rizzuto R, Del Senno L: The cytoplasmic C-terminus of polycystin-1 increases cell proliferation in kidney epithelial cells through serum-activated and Ca^{2+} -dependent pathway(s). *Exp Cell Res* 304: 391–406, 2005
- Cai Y, Maeda Y, Cedzich A, Torres VE, Wu G, Hayashi T, Mochizuki T, Park JH, Witzgall R, Somlo S: Identification and characterization of polycystin-2, the PKD2 gene product. *J Biol Chem* 274: 28557–28565, 1999
- Hanaoka K, Qian F, Boletta A, Bhunia AK, Piontek K,

- Tsiokas L, Sukhatme VP, Guggino WB, Germino GG: Co-assembly of polycystin-1 and -2 produces unique cation-permeable currents. *Nature* 408: 990–994, 2000
24. Luo Y, Vassilev PM, Li X, Kawanabe Y, Zhou J: Native polycystin 2 functions as a plasma membrane Ca²⁺-permeable cation channel in renal epithelia. *Mol Cell Biol* 23: 2600–2607, 2003
 25. Nauli SM, Alenghat FJ, Luo Y, Williams E, Vassilev P, Li X, Elia AE, Lu W, Brown EM, Quinn SJ, Ingber DE, Zhou J: Polycystins 1 and 2 mediate mechanosensation in the primary cilium of kidney cells. *Nat Genet* 33: 129–137, 2003
 26. Yu SP, Kerchner GA: Endogenous voltage-gated potassium channels in human embryonic kidney (HEK293) cells. *J Neurosci Res* 52: 612–617, 1998
 27. Zhu G, Zhang Y, Xu H, Jiang C: Identification of endogenous outward currents in the human embryonic kidney (HEK 293) cell line. *J Neurosci Methods* 81: 73–83, 1998
 28. Berjukow S, Doring F, Froschmayr M, Grabner M, Glossmann H, Hering S: Endogenous calcium channels in human embryonic kidney (HEK293) cells. *Br J Pharmacol* 118: 748–754, 1996
 29. Ukomadu C, Zhou J, Sigworth FJ, Agnew WS: μ 1 Na⁺ channels expressed transiently in human embryonic kidney cells: Biochemical and biophysical properties. *Neuron* 8: 663–676, 1992
 30. Moran O, Nizzari M, Conti F: Endogenous expression of the beta1A sodium channel subunit in HEK-293 cells. *FEBS Lett* 473: 132–134, 2000
 31. Ye C, Rogers K, Bai M, Quinn SJ, Brown EM, Vassilev PM: Agonists of the Ca(2+)-sensing receptor (CaR) activate nonselective cation channels in HEK293 cells stably transfected with the human CaR. *Biochem Biophys Res Commun* 226: 572–579, 1996
 32. Mendez F, Penner R: Near-visible ultraviolet light induces a novel ubiquitous calcium-permeable cation current in mammalian cell lines. *J Physiol* 507: 365–377, 1998
 33. Gunthorpe MJ, Smith GD, Davis JB, Randall AD: Characterisation of a human acid-sensing ion channel (hASIC1a) endogenously expressed in HEK293 cells. *Pflugers Arch* 442: 668–674, 2001
 34. Riccio A, Medhurst AD, Mattei C, Kessel RE, Calver AR, Randall AD, Benham CD, Pangalos MN: mRNA distribution analysis of human TRPC family in CNS and peripheral tissues. *Brain Res Mol Brain Res* 109: 95–104, 2002
 35. Wu X, Babnigg G, Zagranichnaya T, Villereal ML: The role of endogenous human Trp4 in regulating carbachol-induced calcium oscillations in HEK-293 cells. *J Biol Chem* 277: 13597–13608, 2002
 36. Delmas P: Polycystins, calcium signalling, and human disease. *Biochem Biophys Res Commun* 322: 1374–1383, 2004
 37. Garty H, Palmer LG: Epithelial sodium channels: function, structure, and regulation. *Physiol Rev* 77: 359–396, 1997
 38. Tsiokas L, Arnould T, Zhu C, Kim E, Walz G, Sukhatme VP: Specific association of the gene product of PKD2 with the TRPC1 channel. *Proc Natl Acad Sci U S A* 96: 3934–3939, 1999
 39. Robitaille R, Garcia ML, Kaczorowski GJ, Charlton MP: Functional colocalization of calcium and calcium-gated potassium channels in control of transmitter release. *Neuron* 11: 645–655, 1993
 40. Roberts WM, Jacobs RA, Hudspeth AJ: Colocalization of ion channels involved in frequency selectivity and synaptic transmission at presynaptic active zones of hair cells. *J Neurosci* 10: 3664–3684, 1990
 41. Samaranyake H, Saunders JC, Greene MI, Navaratnam DS: Ca(2+) and K(+) (BK) channels in chick hair cells are clustered and colocalized with apical-basal and tonotopic gradients. *J Physiol* 560: 13–20, 2004
 42. Volk T, Schwoerer AP, Thiessen S, Schultz JH, Ehmke H: A polycystin-2-like large conductance cation channel in rat left ventricular myocytes. *Cardiovasc Res* 58: 76–88, 2003
 43. Vandorpe DH, Chernova MN, Jiang L, Sellin LK, Wilhelm S, Stuart-Tilley AK, Walz G, Alper SL: The cytoplasmic C-terminal fragment of polycystin-1 regulates a Ca²⁺-permeable cation channel. *J Biol Chem* 276: 4093–4101, 2001